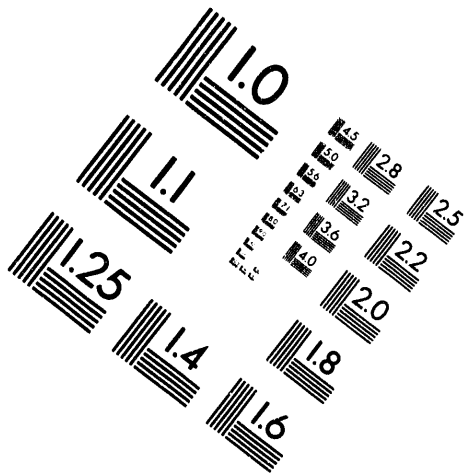




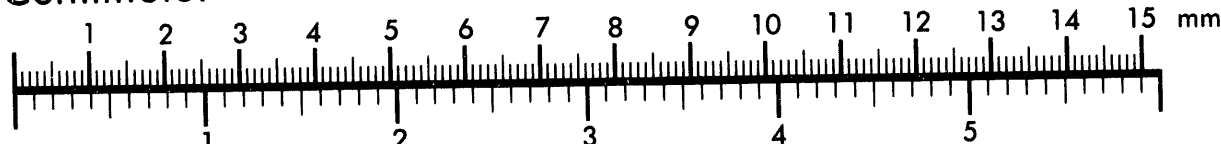
AIM

Association for Information and Image Management

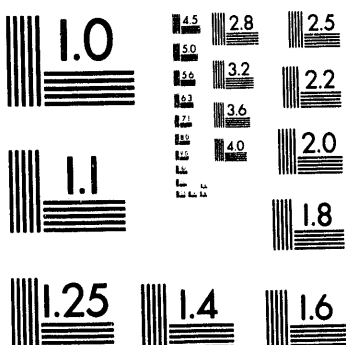
1100 Wayne Avenue, Suite 1100
Silver Spring, Maryland 20910
301/587-8202



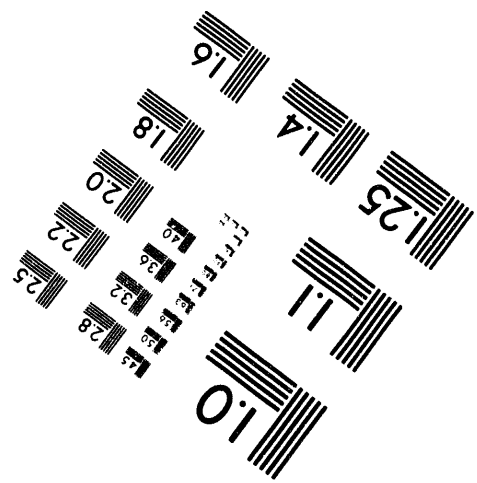
Centimeter

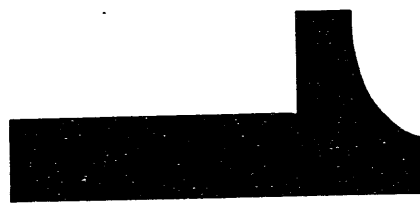
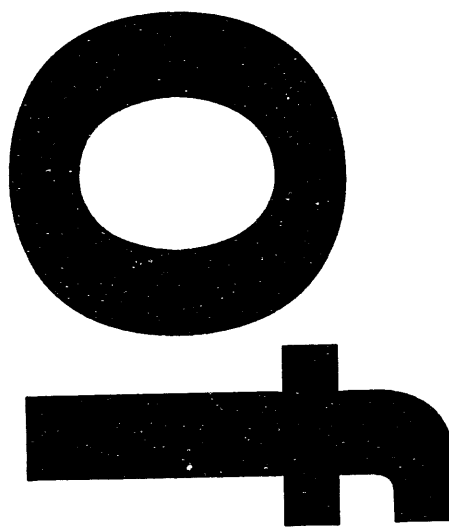


Inches



MANUFACTURED TO AIIM STANDARDS
BY APPLIED IMAGE, INC.





**Investigation of Synchrotron Radiation-Induced Photodesorption in
Cryosorbing Quasi-Closed Geometry**

V. V. Anashin, O. B. Malyshev, and V. N. Osipov

Budker Institute of Nuclear Physics
Novosibirsk, Russia

I. L. Maslennikov and W. C. Turner

Superconducting Super Collider Laboratory*
2550 Beckleymeade Ave.
Dallas, TX 75237

April 1994

*Operated by the Universities Research Association, Inc., for the U.S. Department of Energy under Contract No. DE-AC35-89ER40486.

MASTER

DISTRIBUTION OF THIS DOCUMENT IS UNLIMITED

YPS

Investigation of Synchrotron Radiation-Induced Photodesorption in Cryosorbing Quasi-Closed Geometry

V. V. Anashin, O. B. Malyshev, and V. N. Osipov

Budker Institute of Nuclear Physics

Novosibirsk, Russia

I. L. Maslennikov and W. C. Turner

Superconducting Super Collider Laboratory

Dallas, Texas 75237

Abstract

We report 4.2-K photodesorption experiments in two quasi-closed geometries—a simple tube and a tube with a coaxial perforated liner—designed to measure separately the desorption coefficients of tightly bound and physisorbed molecules. The results are important for the beam tube vacuum of the next generation of superconducting proton colliders that have been contemplated—the 20-TeV Superconducting Super Collider (SSC) in the United States and the 7.3-TeV Large Hadron Collider (LHC) at CERN.

PACS numbers: 29.20.Dh

I. INTRODUCTION

The subject of this paper is the photodesorption of gas molecules in a quasi-closed cryogenic geometry at ~ 4.2 K. Tightly bound molecules in the near surface layer (~ 100 Å) are converted to a steadily increasing surface density of physisorbed molecules by photodesorption and wall pumping. As the physisorbed molecules build up they can undergo thermal- and photodesorption. The gas phase density then consists of three components: the densities of photodesorbed tightly bound and physisorbed molecules not yet readSORBED on the wall, and the isotherm density of the physisorbed molecules. In order to separately measure the photodesorption coefficients of tightly bound and physisorbed molecules we have used two geometries: a simple tube and a tube with a coaxial perforated liner. Except at the earliest moments of photon exposure, gas density in the simple tube is dominated by photodesorption of physisorbed H_2 molecules. With the perforated coaxial liner, physisorbed molecules accumulate behind the liner, where they are shielded from the photon flux, and the gas density is predominantly due to desorption of tightly bound H_2 . We use the term "tightly bound" to include chemical binding and any other form of binding not readily desorbed by warming to room temperature or less.

Although the experiments reported in this paper were originally motivated by the 20-TeV Superconducting Super Collider (SSC) in the United States [1], which is now defunct, the results are important for whatever next-generation superconducting proton collider is eventually built, in particular the 7.3-TeV Large Hadron Collider (LHC) at CERN [2], which is still viable. Indeed, since the SSC was terminated because of a complex web of sociopolitical circumstances while its underlying physics rational remains stronger than ever [3], it seems highly probable that such a next-generation machine will be built. Beyond this there is an ongoing serious effort to examine the parameters of a 100-TeV superconducting proton collider, where synchrotron radiation power and its impact on beam tube vacuum will play an even more dominant role in accelerator design [4]. The beam tubes in these machines are well approximated as closed cryosorbing systems with negligible external pumping and subject to significant fluxes of photodesorbing synchrotron

radiation. Circulating protons will undergo nuclear interactions with gas molecules in the beam tube and will be lost from the beam. Excessive gas density will lead to degraded collider luminosity lifetime and possibly to a runaway increase in beam tube pressure and/or a magnet quench due to the lost beam energy deposited in the cryostats. In the SSC, the saturated isotherm vapor density of H_2 at 4.2 K ($\sim 2 \times 10^{12}/cm^3$) exceeds by a factor of 50 the upper bound allowed by magnet quenching so that accumulation of a monolayer of physisorbed H_2 must be avoided even locally. Since it would be very difficult to work with pure materials or *in situ* cleaning methods in these new colliders, we have used technical materials subjected only to a standard cleaning procedure prior to pump down.

These are the first measurements of photodesorption in a cryosorbing quasi-closed geometry where photodesorption of tightly bound and physisorbed molecules have been clearly separated and the onset of the H_2 isotherm pressure rise has been observed. It is also the first time beam tube conditions anticipated for the SSC have been simulated in enough detail that vacuum modeling predictions can be made. Except for one prior series of experiments [5,6], all previous beam tube photodesorption experiments [7,8,9] have been carried out at room temperature.

II. DESCRIPTION OF THE EXPERIMENTAL APPARATUS

The experiments were performed on a synchrotron radiation beamline of the VEPP2M electron-positron storage ring at the Budker Institute of Nuclear Physics (BINP) in Russia. Electron beam energy and current were set to produce the photon-critical energy and intensity of the SSC (284 eV, $\sim 10^{16}$ photons/m/s). The simple beam tube and bore tube liner were 1-m-long sections of electrodeposited Cu on stainless steel tube (ID = 32 mm, OD = 34.9 mm, Cu thickness = 70 μm). The liner was perforated with 600 2-mm-diameter holes spaced 1 cm axially and 60° azimuthally. The bore tube outside the liner was stainless steel (ID = 41.9 mm, OD = 44.5 mm) welded to the liner with annular rings at the ends. The simple beam tube and the liner bore tube were in turn welded into a horizontal LHe cryostat (~ 20 l LHe) and formed the interface between LHe and vacuum. The beam tube was placed at an angle of 10 mrad to the

synchrotron radiation. Measurements of photon intensity and power at the end of a 1-m beam tube indicated that only $\sim 5\%$ of the incident photons and $\sim 0.5\%$ of the incident power were reflected out the end. The temperature of the liner was not measured. We estimate the temperature rise at the center of the liner to be 5–10 K above the LHe temperature when exposed to a photon intensity of 125–250 mW/m.

Gas densities were measured with calibrated rf quadrupole residual gas analyzers (RGAs) at room temperature. An RGA was connected to the center of the beam tube and at each warm end. The center RGA viewed the beam tube through a 2.4-cm-diameter hole. Care was taken to avoid 4.2-K cryosorbing surfaces in the tube connecting the RGA to the beam tube. The connecting tube is at a right angle to the beam tube and is not directly illuminated by the synchrotron radiation. The connecting tube had a temperature of 77 K at the beam tube hole and made a transition through thin stainless steel bellows to 294 K at the RGA. An annular vacuum gap of ~ 0.2 mm separated the 77-K viewing tube from the 4.2-K beam tube. Thin-wall stainless steel bellows were used at the ends of the 4.2-K beam tube for transitions to 77 K and 294 K. The 294-K vacuum ends of the cryostat were pumped with combination ion and titanium sublimation pumps.

III. DISCUSSION OF THE DATA

The center RGA H_2 pressures with photons on and off are shown versus photon flux in Fig. 1 for the 4.2-K beam tube experiment. The H_2 pressure with photons off was initially $\sim 8 \times 10^{-10}$ Torr until the integrated photon flux reached 1.5×10^{21} photons/m. The H_2 pressure with photons on increased steadily to $\sim 10^{-8}$ Torr at 1.5×10^{21} photons/m. At 1.5×10^{21} photons/m the pump valves at the tube ends were partially closed, and the "on" pressure then increased to a new equilibrium value of 1.0×10^{-7} Torr at 3.75×10^{21} photons/m. The "off" pressure also increased, from the base pressure 9×10^{-10} Torr to an equilibrium value of 6.5×10^{-8} Torr. The rise in the "off" pressure is the increasing isotherm pressure of H_2 cryosorbed to the beam tube. This was verified in two ways: (1) pumping on the helium to reduce the temperature to 3.2 K and observing the pressure drop to the base value, and (2) warming the

tube to 77 K to desorb and pump out the H₂, recooling to 4.2 K, and observing the return to base pressure. The second method is indicated in Fig. 1. The thermally desorbed H₂ was measured to be 3.1×10^{18} H₂/m. After recooling to 4.2 K the beam tube was arranged to expose the opposite side to photons. Opening the photon shutter again resulted in a steady increase in H₂ pressure, now to a new equilibrium value of $\sim 2.0 \times 10^{-8}$ Torr. At the end of the second exposure an additional integrated photon flux of 5.25×10^{21} photons/m had been accumulated, and the thermally desorbed H₂ was 2.2×10^{18} H₂/m. The H₂ isotherm pressure of 6.5×10^{-8} Torr at the end of the first exposure was less than the saturated value of $\sim 5 \times 10^{-6}$ Torr because of axial diffusion to the end pumps. In room-temperature photodesorption experiments, the side of the tube opposite direct illumination has been observed to be subjected to a desorbing flux of diffusely scattered photons. The conditioning of the indirectly illuminated surface was equivalent to approximately 25% of the direct illumination [10,11]. Here, because of cryosorption, exposing the side opposite direct illumination would have to have been done with the liner configuration rather than the simple beam tube to make a similar quantitative statement. The opposite side exposure of the simple beam tube was done here mainly to check systematic behavior and to ensure that everything was working properly; this was confirmed, since results from illumination of both sides of the beam tube in Fig. 1 are similar.

For the liner experiment, pressures with photons off were constant (5×10^{-10} Torr H₂ and 1.5×10^{-10} Torr CO) and have been subtracted (Fig. 2). The dynamic H₂ pressure started at a quasi-steady value of 2×10^{-9} Torr until an integrated photon flux of 3.7×10^{20} photons/m was reached, at which point the pressure increased to a new equilibrium value of 1.5×10^{-8} Torr by 6.0×10^{20} photons/m. This increase was the isotherm pressure of H₂, now cryosorbed on the bore tube. H₂ had accumulated on the 4.2-K bore tube until the isotherm reached the pressure inside the liner. The bore tube surface then ceased to pump, and the remaining pumping was by axial diffusion to the ends of the tube. The ratio of the liner hole pumping speed to the axial conductance of the liner and end connections is in agreement with the observed increase in pressure by a factor of 7.5. The H₂ isotherm assertion was verified in three ways, as indicated in Fig. 2:

(1) there was no change in the CO pressure, (2) at 1.2×10^{21} photons/m the pump valves were partially closed and the H₂ pressure increased to 3×10^{-8} Torr, and (3) the helium was pumped to reduce the LHe temperature to 3.2 K, whereupon the H₂ isotherm pressure dropped to a negligible value, the bore tube reverted to pumping, and the H₂ pressure decreased to $\sim 1 \times 10^{-9}$ Torr at 1.64×10^{21} photons/m. At 1.64×10^{21} and 3.8×10^{21} photons/m the LHe dewar had to be refilled, causing momentary increases in temperature and pressure. At 6.5×10^{21} photons/m the cryostat was warmed to 77 K and the thermally desorbed H₂ was 8.2×10^{18} H₂/m. The cryostat was recooled to 4.2 K, and exposure continued to 8.0×10^{21} photons/m; then the cryostat was cooled to 3.2 K and exposure continued to 9.1×10^{21} photons/m. At the conclusion of the run the cryostat was again warmed and the thermally desorbed H₂ was measured to be 1.9×10^{18} H₂/m. Except as noted, there was an overall trend for the normalized H₂ pressure to decrease from its initial value of 2×10^{-9} Torr to 2.5×10^{-10} Torr at 9.1×10^{21} photons/m. The relative decrease of CO pressure was less, from 3×10^{-10} Torr to 1.3×10^{-10} Torr.

There are some additional features in Figs. 1 and 2 that we have yet to explain, in particular the pressure bumps in Fig. 1 at 6×10^{21} photons/m, and in Fig. 2 at 5×10^{21} photons/m and 7.7×10^{21} photons/m. These were due to interruption of synchrotron radiation for periods of one hour up to two days.

The data will now be interpreted in terms of molecular desorption coefficients per incident photon. Under rather general conditions, if the desorption coefficient of physisorbed molecules (η') is large compared to the desorption coefficient of tightly bound molecules (η), the dynamic density of gas molecules in a cryosorbing beam tube (4.2-K beam tube or liner) is related to η' by [12]

$$\eta' \dot{\Gamma} = \sigma_w A_w \frac{\bar{v}_1}{4} n_1 = \sigma_w A_w \frac{\bar{v}_2}{4} n_2, \quad (1)$$

where $\dot{\Gamma}$ = photons/m/s, σ_w is the sticking coefficient, A_w the beam tube wall area per unit length, \bar{v} the effective mean molecular speed, n the dynamic molecular gas density, and subscripts "1" and "2" refer to the 4.2-K beam tube and 294-K RGA, respectively. The second equality

follows from flux balance $n_1\bar{v}_1 = n_2\bar{v}_2$ between the beam tube and RGA. The condition $\eta' \gg \eta$ is already evident from the relative magnitude of pressures in Figs. 1 and 2 and will be verified below except at the earliest moments of photon exposure. Although \bar{v}_1 isn't known, it is reasonably certain that the molecules inside the RGA had reached equilibrium with the 294-K walls so $\bar{v}_2(H_2) = 1.76 \times 10^5$ cm/s. From eq. (1), measurement of the pressure is equivalent to measurement of η'/σ_w . At low-surface coverage the desorption coefficient η' is expected to depend linearly on the surface density s of cryosorbed molecules; $\eta' = \eta'_0(s/s_m)$, where we have normalized the surface density to a "monolayer": $s_m = 3 \times 10^{15}$ molecules/cm².

For the liner experiment, the molecular density s cryosorbed to the liner surface reaches a quasi-steady state, the surface ceases to pump, and we have the following equation describing pumping by the holes:

$$\eta \dot{\Gamma} = p N_h A_h \frac{\bar{v}_1}{4} n_1 = p N_h A_h \frac{\bar{v}_2}{4} n_2, \quad (2)$$

where η is the desorption coefficient of tightly bound molecules not previously photodesorbed and specifically excludes desorption of physisorbed molecules, N_h = number of holes/m, A_h = area of a hole, and p is the molecular transmission probability through a hole. Eq. (1) is valid here also and now gives a relation between η and η' : $\eta'(s)/\sigma_w = (A_w/p N_h A_h) \eta$. This relation is not useful for measurement of η' but can be used to estimate the self-consistent surface density of physisorbed H₂ on the liner once the parametric dependence of η' on s is known. The liner experiment is useful for determining η , while the 4.2-K beam tube experiment is useful for determining η' versus s . The coefficient η corresponds to what is usually measured in room-temperature photodesorption experiments [7,8,9], although here the tube is near 4.2 K. The validity of eq. (2) depends on two approximations that are valid here: the axial conductance of the beam tube is negligible compared to the liner hole conductance, and the liner hole conductance is negligible compared to the pumping speed of the 4.2-K bore tube surface. From eq. (2) the measurement of dynamic pressure with a liner is equivalent to measurement of η . A more complete analysis of photodesorption in a cold beam tube and eqs. (1) and (2) is given in ref. 12.

The H_2 desorption coefficient η'/σ_w versus photon flux is given in Fig. 3(a) for the dynamic pressure component (photons on minus off) of Fig. 1. The $s(H_2)$ dependence of η'/σ_w is shown in Fig. 3(b), inferred from an earlier 4.2-K beam tube experiment for which we had directly measured the H_2 isotherm pressure versus s prior to exposure to photons [13]. The data in Fig. 3(b) are reasonably well approximated by a linear dependence $\eta' = \eta'_0(s/s_m)$ and $\eta'_0/\sigma_w = 7.0 \pm 1.5$, valid at least over the range $0 \leq s/s_m \leq 1$. Although we don't yet have measurements of σ_w , it is impressive how large η' can be for reasonable guesses (say, $\sigma_w \approx 0.1$ to 1.0, $\eta'_0 \approx 0.7$ to 7.0).

The desorption coefficients $\eta(H_2)$ and $\eta(CO)$ versus integrated photon flux are given in Fig. 4, using a hole transmission probability $p = 0.59$ and neglecting sticking on the walls of the holes. H_2 and CO data are also shown for room-temperature data from a similar electrodeposited Cu beam tube. The room temperature coefficients appear somewhat larger than 4.2 K coefficients. However, except for what appear to be initial temperature dependent transients most apparent in CO in Fig. 8, more careful experiments would be required to determine if this is a real effect or due to other differences between the experiments. The two experiments were done with different samples of beam tube and the room temperature data was taken in a high intensity beamline with eight times higher photon intensity than the 4.2 K data. We estimate the total numbers of desorbed molecules by integrating desorption coefficients over the measured range of integrated photon flux $\Gamma = 9 \times 10^{21}$ photons/m: for the 4.2-K data, $1.1 \times 10^{19} H_2/m$ and $9.2 \times 10^{17} CO/m$; for the 294-K data, $3 \times 10^{19} H_2/m$ and $5 \times 10^{18} CO/m$. The 4.2-K data are in reasonable agreement with the measurements of thermally desorbed H_2 : $1.0 \times 10^{19} H_2/m$. Comparing the magnitudes of η and η' coefficients for H_2 , the desorption of physisorbed H_2 will dominate the total dynamic H_2 pressure in a 4.2-K beam tube except at the very earliest moments of photon exposure.

Prior to the work reported in this paper the only previous 4.2-K photodesorption data were from the two experiments reported in refs. 5 and 6. These experiments were carried out in the 1980s as part of the SSC Central Design Group effort preceding approval to begin construction. The first experiment was in quasi-closed geometry with a 5-m-long, 4.2-K stainless steel and

electroplated Cu beam tube similar to that used here; the second experiment was in open geometry with small samples cut from the beam tube. The underlying philosophy was to measure the 4.2-K desorption coefficients of tightly bound molecules in open geometry and the effect of loosely bound physisorbed molecules in quasi-closed beam tube geometry. A liner configuration was not employed. It is of interest to compare the results obtained in this paper with those in refs. 5 and 6; we now turn to a brief discussion of this comparison.

In the 4.2-K beam tube experiment of ref. 5 the RGA pressure rise was reported as a function of integrated photon flux, and no attempt was made to reduce the data in terms of the desorption coefficient of physisorbed H₂. However, the fact that the pressure increased with integrated photon flux, as in Fig. 1 and unlike room-temperature experiments, implies basic agreement with the notion that physisorbed H₂ is building up and making a significant contribution to the 4.2-K beam tube density. The only question then is whether the magnitudes of the effect agree. We compare the density increase of H₂ at the maximum integrated photon flux 10²¹ photons/m in ref. 5 with the data in Fig. 1. At a photon flux 10¹⁶ photons/m/s and integrated flux 10²¹ photons/m, the density increase of H₂ inside the 4.2-K beam tube of ref. 5 was typically $3.3 \times 10^9/\text{cm}^3$ [14]; for the same photon intensity and integrated flux the two runs in Fig. 1 give H₂ beam tube densities of $1.7 \times 10^9/\text{cm}^3$ and $3.6 \times 10^9/\text{cm}^3$. Given the many differences in experimental technique and calibration we think this is reasonable agreement. The case that the increase in H₂ density is actually due to photodesorption of physisorbed H₂ is, however, much stronger in our experiment than in ref. 5.

We now turn to comparison of desorption coefficients of tightly bound H₂ at 4.2-K, measured in open sample geometry in ref. 6 and in quasi-closed beam tube liner geometry here. There are legitimate reasons for questioning the validity of comparison of photodesorption coefficients measured in open sample and beam tube experiments: diffusely scattered photons contribute significantly to desorption from a beam tube surface but not from an open sample; the detailed profiles of surface illumination intensity may vary greatly; photon impact may create active sights for tightly bound molecules; desorption coefficients for open samples are presented as a

function of photons per unit area, whereas beam tube experiments use photons per unit length, etc. Nevertheless we will compare the photodesorption coefficients of Fig. 4 to the open sample results of ref. 6, assuming the beam tube is uniformly illuminated. With this assumption 10^{21} photons/m is equivalent to 10^{18} photons/cm²; this same assumption was made in ref. 6 for comparing 4.2-K and room-temperature open sample data to room-temperature beam tube data in ref. 5. From Fig. 4 η (H₂, 4.2 K) = 2.5×10^{-3} at 10^{21} photons/m. From Fig. 6 in ref. 6, an average over three open samples gives η (H₂, 4.2 K) = 3.8×10^{-3} at 10^{18} photons/cm². The two results are within a factor of two; given the very different approaches, this is perhaps as good an agreement as could be hoped for.

IV. CONCLUSIONS AND SUMMARY

For the SSC it seems that a simple 4.2-K beam tube of the electrodeposited Cu used in these experiments would entail an operationally inconvenient number of beam tube warm-ups to keep the pressure within a tolerable range: 3.4 monolayers of H₂ were desorbed in the equivalent of 10.4 days of operation at design intensity. The liner configuration equipped with cryosorber would circumvent this difficulty. In order to estimate the luminosity lifetime with the liner it is necessary to know the mean molecular velocity \bar{v}_1 in eq. (2). A lower bound on the mean velocity corresponds to the 4.2-K temperature of the cryostat. In that case and for the liner used here the luminosity lifetime due to scattering on H₂ and CO would exceed the 150-h vacuum design goal after $\sim 9 \times 10^{21}$ photons/m or 10 days of operation. Compared to a smooth beam tube, a liner with perforations increases the impedance seen by the circulating proton beam and reduces the safety margin for beam instabilities. However, the impedance of a liner similar to that investigated here has been measured and appears to allow a comfortable safety margin for beam instabilities [15].

ACKNOWLEDGMENTS

We would like to thank A. Skrinsky for valuable discussions and encouraging support given to this work. We would also like to thank the VEPP2M operating crew for their expertise running the storage ring up to ten times normal beam current. We are indebted to Myron Strongin for valuable comments. The Superconducting Super Collider Laboratory is operated by the Universities Research Association, Inc., for the U.S. Department of Energy under Contract No. DE-AC-35-89ER40486.

REFERENCES

- [1] Conceptual Design of the Superconducting Super Collider, J.D. Jackson, ed., SSC-SR-2020 (1986).
- [2] Design Study of the Large Hadron Collider, LHC Study Group, CERN 91-03 (1991).
- [3] D. Ritson, "Demise of the Texas Supercollider," *Nature*, **236**, 607, 16 Dec. 1993.
- [4] E. Keil, "Scaling Laws and Cost Optimization for Hadron Colliders Around 100 TeV," *Proc. of 19th Eloisatron Workshop, Erice, Italy, 13–19 Nov. 1991*.
- [5] D. Bintinger, P. Limon, H. Jostlein, and D. Trbjovic, "Status of the SSC Photodesorption Experiment," *SSC-102* (1986).
- [6] D. Bintinger, P. Limon, and R. Rosenberg, *J. Vac. Sci. Technol.*, **A7**, 59 (1989).
- [7] C. Foerster, H. Halama, and C. Lanni, *J. Vac. Sci. Technol.*, **A8**, 2856 (1990).
- [8] A. G. Mathewson, O. Grobner, P. Strubin, P. Marin, and R. Souchet, *American Vacuum Society Series 12, Conference Proceedings No. 236*, p. 313 (1991).
- [9] I. Maslennikov, W. Turner, V. Anashin, O. Malyshev et al.; "Photodesorption Experiments on SSC Collider Beam Tube Configurations," *SSCL-Preprint 378* (1993). *Proc. of 1993 IEEE Part. Acc. Conf., Washington, D.C.*, p. 3876 (1993).
- [10] A. Mathewson, M. Andritschky, O. Grobner, F. Schumann, R. Souchet, and P. Strubin, "Gas Desorption and Surface Conditioning of a Synchrotron Radiation Source," *Proc. of Topical Conf. on Vacuum Design of Advanced and Compact Synchrotron Light Sources, Brookhaven National Laboratory, Upton, New York, May 16–18, 1988. CERN-LEP-UA 88-08*.
- [11] C. Foerster, C. Lanni, I. Maslennikov, and W. Turner, "Photon Desorption Measurements of Copper and Copper Plated Beam Tubes for the SSCL - 20 TeV Proton Collider." To appear in *Proc. of the 40th National Symposium of the American Vacuum Society, Nov. 15–19, 1993, Orlando, Florida*.

- [12] W. Turner, "Dynamic Vacuum in the Beam Tube of the SSCL Collider—Cold Beam Tube and Liner Options," SSCL-Preprint 404 (1993). Proc. of 1993 IEEE Part. Acc. Conf., Washington, D.C., p. 3833 (1993).
- [13] V. Anashin, A. Evstigneev, O. Malyshev, V. Osipov, I. Maslennikov, and W. Turner, "Summary of Recent Photodesorption Experiments at VEPP2M," SSCL-N-825 (1993).
- [14] Site Specific Conceptual Design of the Superconducting Super Collider, J.R. Sanford and D.M. Matthews, eds., SSCL-SR-1056 (1990), p. 241.
- [15] E. Ruiz, L. Walling, Y. Goren, and N. Spayd, "Beam Coupling Measurements and Simulations of a Beam Pipe Liner with Pumping Holes or Slots," SSCL-Preprint 351 (1993). Proc. of 1993 IEEE Part. Acc. Conf., Washington, D.C., p. 3405 (1993).

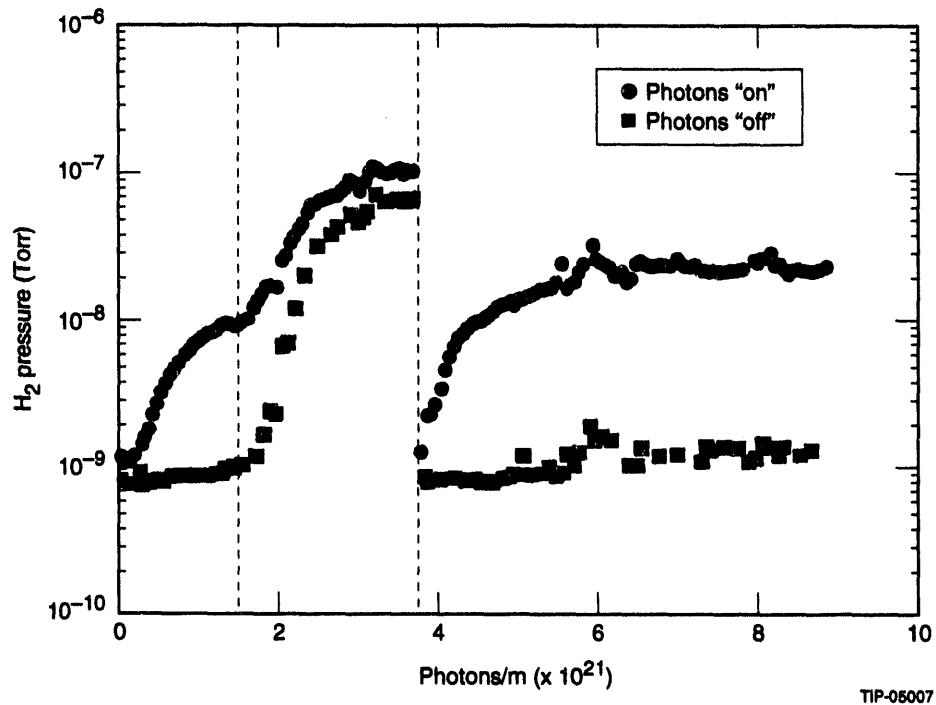


FIG. 1: Room temperature RGA H₂ pressure measured at the center of the 4.2-K beam tube versus integrated photon flux with photons on and photons off. The raw pressure difference "on" minus "off" has been normalized to 1×10^{16} photons/m/s. The vertical dashed lines correspond to features discussed in the text.

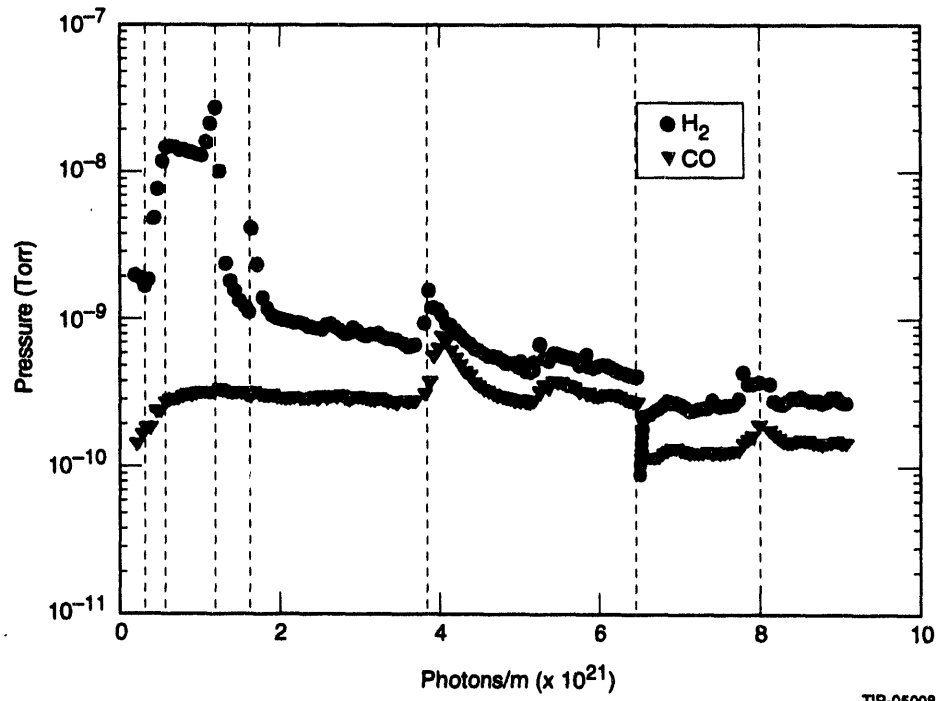
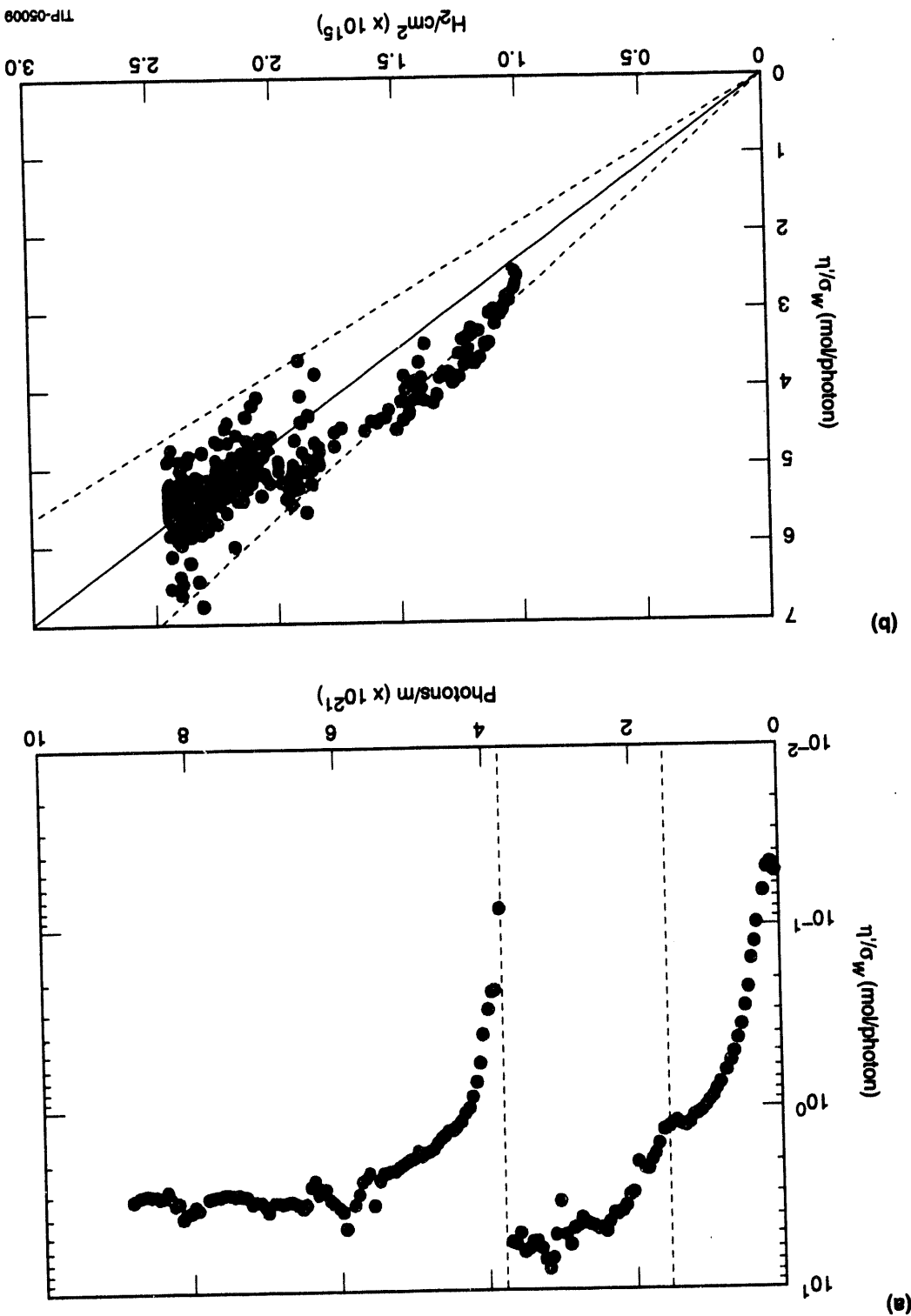


FIG. 2: Room temperature RGA H₂ and CO dynamic pressures measured at the center of the liner configuration. Dynamic pressure is normalized to 1×10^{16} photons/m/s.

FIG. 3: (a) η'/G_{v} versus photon flux and (b) versus the surface density of cryosorbed H_2 .



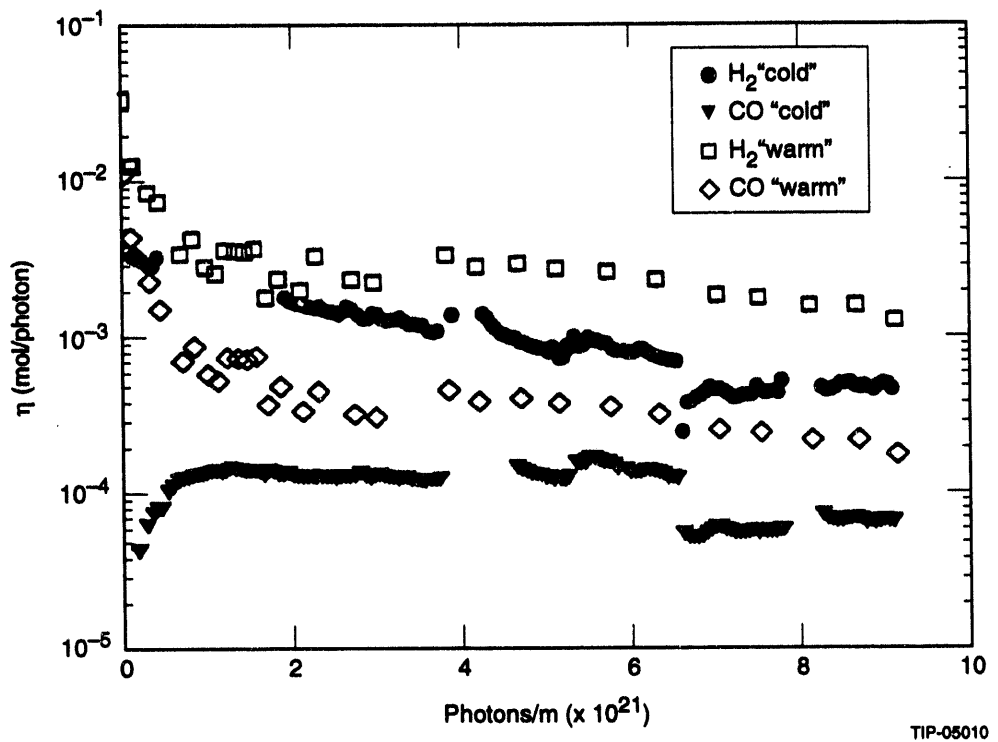


FIG. 4: $\eta(\text{H}_2)$ and $\eta(\text{CO})$ versus integrated photon flux.

100-25

9/11/96
FILED
DATE

